

Article

Inorganic Sorbents for Wastewater Treatment from Radioactive Contaminants

Natalya A. Nekrasova, Vitaly V. Milyutin, Victor O. Kaptakov and Evgeny A. Kozlitin *

Frumkin Institute of Physical Chemistry and Electrochemistry of the Russian Academy of Sciences (IPCE RAS), Bld. 4, 31 Leninsky Prospect, 119071 Moscow, Russia; nnekrassova@gmail.com (N.A.N.); vmilyutin@mail.ru (V.V.M.); v.kapt@yandex.ru (V.O.K.)

* Correspondence: evgeny_kozlitin@mail.ru

Abstract: The article presents the distribution coefficient (K_d) values of ^{137}Cs and ^{90}Sr tracer radionuclides in solutions of sodium and calcium salts for a wide range of commercially available inorganic sorbents: natural and synthetic aluminosilicates, manganese, titanium and zirconium oxyhydrates, titanium and zirconium phosphates, titanosilicates of alkali metals, and ferrocyanides of transition metals. The results were obtained using a standard technique developed by the authors for evaluating the efficiency of various sorption materials towards cesium and strontium radionuclides. It was shown that bentonite clays and natural and synthetic zeolites are the best for decontaminating low-salt natural water from cesium radionuclides, and ferrocyanide sorbents are the choice for decontaminating high-salt-bearing solutions. The manganese (III, IV) oxyhydrate-based MDM sorbent is the most effective for removing strontium from natural water; for seawater, the barium silicate-based SRM-Sr sorbent is the first-in-class. Results of the study provide a possibility of making a reasonable choice of sorbents for the most effective treatment of natural water and technogenic aqueous waste contaminated with cesium and strontium radionuclides.

Keywords: cesium and strontium radionuclides; liquid radioactive waste; radioactively contaminated aqueous streams; decontamination



Citation: Nekrasova, N.A.; Milyutin, V.V.; Kaptakov, V.O.; Kozlitin, E.A. Inorganic Sorbents for Wastewater Treatment from Radioactive Contaminants. *Inorganics* **2023**, *11*, 126. <https://doi.org/10.3390/inorganics11030126>

Academic Editor: Hans-Conrad zur Loye

Received: 20 February 2023

Revised: 12 March 2023

Accepted: 14 March 2023

Published: 16 March 2023



Copyright: © 2023 by the authors. Licensee MDPI, Basel, Switzerland. This article is an open access article distributed under the terms and conditions of the Creative Commons Attribution (CC BY) license (<https://creativecommons.org/licenses/by/4.0/>).

1. Introduction

The production and application of radionuclide-containing materials generate liquid radioactive waste (LRW) of various chemical compositions and activity levels. LRW presents the most severe potential environmental hazard due to its large volume and high total activity. Furthermore, during radiation accidents at the nuclear fuel cycle facilities, an uncontrolled release and migration of radioactive substances result in environmental pollution. As such, the radiation accidents at the Chernobyl Nuclear Power Plant of the USSR, in 1986 [1] and Fukushima-1 Nuclear Power Plant of Japan, in 2011 [2] brought an enormous environmental damage. Therefore, developing and upgrading techniques for decontaminating liquid radioactive waste and radioactively contaminated natural water is an important and challenging issue.

Physical adsorption and ion exchange-based sorption methods adopt a high profile among the physicochemical methods used for decontaminating aqueous solutions from toxic and radioactive impurities. Physical adsorption methods with various types of adsorbents, primarily active carbons, are mainly used at the initial stages of polluted water treatment to remove oil products, surfactants, uranium, and heavy metals [3–7].

Since radionuclides in aqueous solutions, basically, exist as simple or partially hydrolyzed aqua-ionic species, they can be removed by ion-exchange techniques using organic ion exchange resins and natural and synthetic inorganic sorbents of various types.

Organic ion exchange resins are commercially available products that possess high sorption, kinetic, and performance characteristics and are widely used to remove toxic components from waste effluents.

Strongly acidic sulfonic cation exchangers are most widely used in industrial practice. This type of ion exchanger is characterized by an increase in affinity with an increase in the charge and size of the adsorbed ion. However, in general, their selectivity, in particular to cesium and strontium radionuclides, in the presence of interfering cations is low; hence, they are used for decontamination of low salt-bearing solutions only [8,9].

Medium acid phosphate cation exchangers, weak acid carboxyl cation exchangers, and chelate ion exchangers with iminodiacetate and phosphonic groups exhibit a high selectivity to uranium, thorium, and nonferrous metal ions. It is possible to use these type of ion exchangers to selectively remove the above impurities against the background of the prevailing bulk amounts of alkali and alkaline earth metal ions [10–12].

Whereas radionuclides in the wastewater composition exist substantially as the cationic species, anion exchangers are currently still employed to recover uranium from sulfuric acid and carbonate solutions, where uranium exists in the form of complex anionic species [13,14].

Ion exchange resins are commercially produced by several companies, namely, Dow Chemical, USA, Rohm&Haas, USA, Lanxess, Germany, Purolite, Great Britain. In Russia, the ion exchange resins are manufactured at the LLC Production Association "TOKEM" (LLC PO "TOKEM"), Kemerovo, and JSC "Axion-Rare and Precious Metals" (JSC "ARPM"), Perm.

Because of limited selectivity and high cost, exhausting organic ion-exchange resins are reused by the regeneration with solutions of inorganic acids or salts. The experience gained in the operation of ion-exchange plants and technical and economic calculations showed that the application of the ion exchange technique with organic ion exchangers is reasonable merely for the treatment of water containing no more than 1 g dm^{-3} of dissolved salts. The higher the salt content, the more frequent regeneration of ion exchangers is required generating significant volumes of secondary liquid radioactive waste.

To date, inorganic sorbents of various types are widely used to remove radioactive contaminants from LRW and natural water. Among them are natural aluminosilicates (clays) [15–18]; zeolites of natural and artificial origin [19–23]; oxyhydrate sorbents [24–27]; titanium and zirconium phosphates [28,29]; alkali metal titanates and titanosilicates [30–35]; transition metal ferrocyanides [36–38]; and other types of sorbents. These sorbents are primarily used to remove long-lived cesium and strontium radionuclides that most of the time define the total LRW radioactivity.

Unlike the organic ion exchangers, inorganic sorbents exhibit increased selectivity to certain ions, high chemical and thermal resistance, and radiation stability. The selectivity of inorganic sorbents is associated primarily with the so-called "zeolite effect", which, in its turn, is explained in terms of a close match between an adsorbed ion size and that of the entry windows in the sorbent crystal lattice [39–42].

The sorption of ions on inorganic sorbents is a complex and multistage process: in the first stage, the adsorbed ions move from the solution to the external surface of the granule, then they diffuse in the pores of the granule to the crystallites of the solid phase. Finally, the diffusion of the ion into the crystal lattice of the sorbent occurs. For cesium, the phenomenon of "zeolite effect" pronounces itself most in the transition metal ferrocyanides, synthetic and natural zeolites, as well as for strontium in the MDM sorbent based on manganese oxides. The presence of large macro- and mesopores makes the developed porous structure and contributes to the rapid transport of adsorbed ions to the surface of the sorbing phase. In other words, they are responsible for the kinetic characteristics of the process. Thus, the large-pore silica-gel-based FSS sorbent has faster cesium sorption kinetics than the sorbents of microporous structures, such as zeolites. In our paper, we highlighted the applied aspects of various inorganic sorbents for removing highly toxic cesium and strontium radionuclides from aqueous solutions. The selectivity and sorption mechanism-related issues are discussed in [43–45].

The capability of inorganic sorption materials to selectively adsorb cesium and strontium radionuclides is widely employed for the treatment of LRW and radioactive natural

water of various compositions [32,46–48] and for creating engineered geochemical barriers around the radioactive waste storage facilities [46,49,50].

Despite a significant number of works and reviews devoted to the sorption studies of cesium and strontium on various sorption materials, the reported sorption characteristics were determined under various experimental conditions, which does not allow an objective comparison of the sorbent efficiency for removing cesium and strontium from solutions.

In that regard, this work pursued the characterization studies of different types of sorption materials most effective for the sorption of cesium and strontium radionuclides, the primary radioactive contaminants in the LRW and natural water composition. First-of-all, attention was given to those commercially available and currently produced on an industrial or pilot scale. In the last 5–10 years, no new types of sorbents have appeared superior in selectivity to those known before.

The novelty of our work is the comparative testing of various types of sorbents for the sorption of cesium and strontium radionuclides based on a standardized technique developed in our laboratory. This technique provides an objective comparison of the available sorbents' sorption characteristics for a particular application.

2. Results and Discussion

In Table 1, the distribution coefficient (K_d) values for ^{137}Cs and ^{90}Sr radionuclides are given for various types of sorbents. The values were calculated as an average of 2–3 parallel experiments; the relative error in determining the K_d value did not exceed 10%.

Table 1. The distribution coefficient (K_d) values for ^{137}Cs and ^{90}Sr on different sorbent types.

Sorbent Type	Brand Name, Designation	K_d ^{137}Cs , $\text{cm}^3 \text{g}^{-1}$ in 0.1 mol dm^{-3} NaNO_3	K_d ^{90}Sr , $\text{cm}^3 \text{g}^{-1}$ in 0.01 mol dm^{-3} CaCl_2
Sulfonic cation exchanger	Purolite C 100	450	290
Bentonite clay	Bent-Ru	9100	40
Bentonite clay	Bent-Gr	2300	35
Clinoptilolite	Cl-UKR	1600	70
Clinoptilolite	Cl-RUS	1800	65
Zeolite of type A	NaA	8900	350
Zeolite of type X	NaX	1800	320
Zirconium(IV) oxyhydrate	Termoksid-3K	150	210
Manganese (III, IV) oxyhydrate	MDM	290	5600
Zirconium phosphate	Termoksid-3A	1800	440
Nickel-potassium ferrocyanide	Termoksid-35	1.2×10^5	35
Nickel-potassium ferrocyanide	FNS	8.4×10^4	10
Nickel-potassium ferrocyanide	FND	8.1×10^4	25
Barium silicate	SRM-Sr	<10	185
Activated charcoal	BAU	440	<5
Activated charcoal	NWC	470	<5

The results presented in Table 1 show that in an 0.1 mol dm^{-3} NaNO_3 -containing low-salt-bearing solution, bentonite clays, natural and synthetic zeolites, zirconium phosphate, and ferrocyanide sorbents exhibited an increased selectivity to ^{137}Cs , with a K_d of ^{137}Cs

$>10^3 \text{ cm}^3 \text{ g}^{-1}$. Conversely, sulfonic cation exchangers, oxyhydrate, and charcoal sorbents showed relatively low selectivity to cesium.

As mentioned earlier, the selectivity of sorption on inorganic sorbents is associated with the so-called “zeolite” effect, when the complete sorption is observed if the sizes of the entrance windows in the crystal structure of the sorbents and absorbed ions are close.

As shown in Table 1, bentonite clays are effective for the selective sorption of cesium. Sorption characteristics of this type of clay are associated mainly with minerals of the smectite group (illite, montmorillonite) in their composition [51]. The selectivity of sorption, in this case, is associated with the possibility of replacing cations in the interlayer space with Sr^{2+} , Ba^{2+} , Rb^+ , or Cs^+ having the ion radius in the range from 1.75 to 2.02 Å (Figure 1) [52].

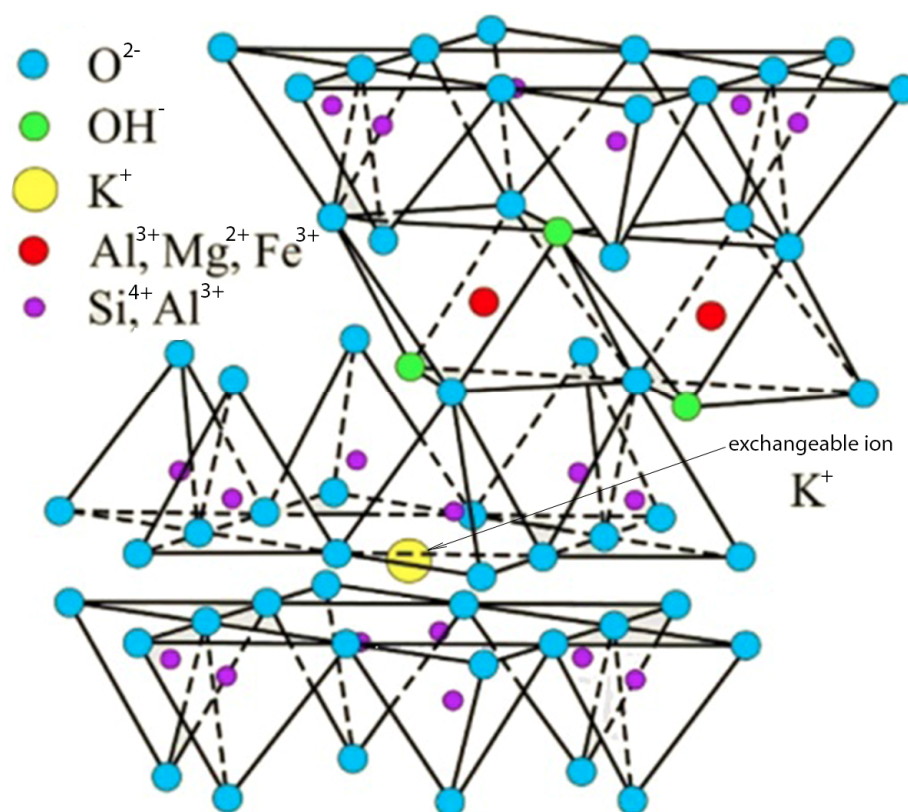


Figure 1. Crystal structure of illite. The exchangeable ion is K^+ .

Sorption of cesium on clay minerals occurs by the ion exchange mechanism; interplanar layers of clay minerals exchange their mobile ions with the liquid phase. The exchangeable ions in the interlayer space can be Na^+ , K^+ , Ca^{2+} , and Mg^{2+} ; as an example, Figure 1 shows the illite mineral, where the exchanging ion is K^+ . In Figure 1, it is indicated by an arrow.

The selectivity series for alkali metals during sorption on bentonite clays is as follows: $\text{Cs}^+ < \text{Rb}^+ < \text{K}^+ < \text{Na}^+$, which indicates a high selectivity of the material in question to cesium ions [53].

In the sorption on clays, the surface structure is of great importance. For example, bentonite clay particles (Bent–Ru sorbent) are mainly hexagonal-shaped, with the predominant size in the range of 10–100 nm (Figure 2). The block structure of illite particles contributes to the formation of a rather large specific surface area of $22 \pm 1 \text{ m}^2 \text{ g}^{-1}$, defining the high degree of radionuclide sorption from aqueous solutions [54].

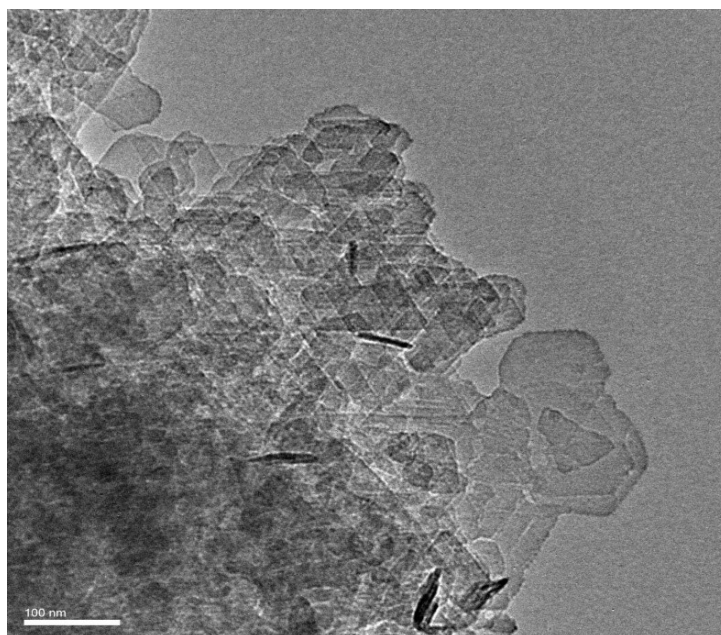


Figure 2. Scanning electron micrograph/image of bentonite clay particles (SEM analysis data).

The zeolite effect manifests itself to the greatest extent during the sorption of cesium on transition metal ferrocyanide-based sorbents.

Divalent transition metal ferrocyanides are formed due to the interaction between a soluble transition metal salt and alkali metal (sodium, potassium) ferrocyanides. Depending on the ratio of the reacting components, precipitates of mixed transition metal ferrocyanides of the general formula of $\text{Me}^{\text{I}}_{4-2x}\text{M}^{\text{II}}_x[\text{Fe}(\text{CN})_6]$ are formed, where Me(I) denotes Na or K, and M (II) is the divalent transition metal ion, namely, Cu, Ni, Co, Zn, etc. The tendency of alkali metal ions to enter the composition of transition metal ferrocyanides increases with an increase in the ionic radius of an alkali metal [55].

Mixed transition metal ferrocyanides have a face-centered cubic lattice consisting of a poly-anion framework that contains equal amounts of M (II) and Fe (II) transition metal ions located at the lattice sites. In an octahedral arrangement around the iron atoms, CN-groups oriented in the direction of the transition metal atoms make bridges. Some transition metal ions M (II) and alkali metal ions Me (I) are located in the center of the cubic lattice octants (Figure 3, [55]).

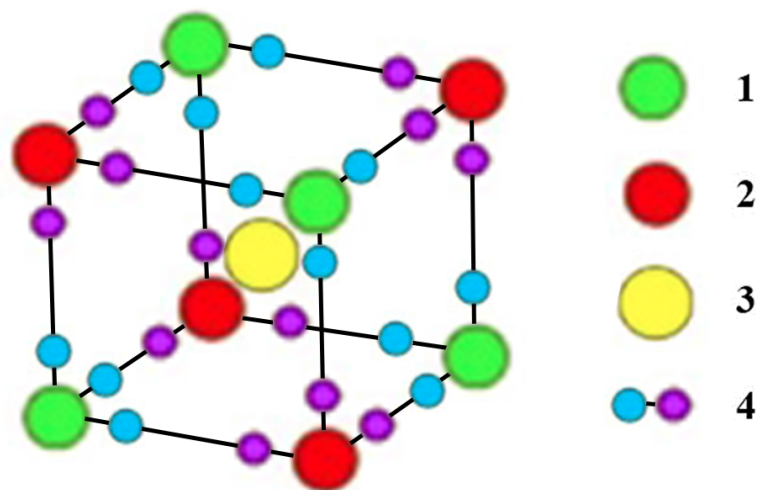


Figure 3. A crystal structure model of mixed ferrocyanides. 1—Me (II); 2 is Fe (II); 3 is Me (I); 4 is C-N.

The ion-exchange properties of ferrocyanides are attributed to their ability for an equivalent replacement of mobile alkali metal cations located in the center of the lattice.

The entrance windows' size in the lattice of mixed transition metal ferrocyanides ranges from 3.3 to 3.5 Å, which is very close to the size of the cesium ion ($r_i = 1.65$ Å). When a Cs^+ ion enters the lattice, the close coincidence of sizes leads to a strong dispersion interaction and, accordingly, the high selectivity to cesium. The selectivity series for mixed transition metal ferrocyanides is the following: $\text{Cs}^+ < \text{Rb}^+ \ll \text{K}^+ \ll \text{Na}^+$ [56].

The fine-crystalline nature of mixed ferrocyanide precipitates does not enable their application for cesium sorption in a flow mode. Therefore, several methods were used to obtain granular sorbents. The first one consists in depositing a layer of transition metal ferrocyanide precipitate on a porous inorganic matrix with a high specific surface area (silica gel, aluminosilicate). In particular, the FNS sorbent, nickel–potassium ferrocyanide, deposited on the surface of large-pore silica gel belongs to this group. The second granulation method is based on the sol-gel process; it includes fabricating a spheric gel of the corresponding metal oxyhydrate followed by sequential treatment of it with solutions of a transition metal salt and potassium ferrocyanide. According to this technology, the nickel–potassium ferrocyanide-based Termoksid-35 sorbent and zirconium oxyhydrate-based Termoksid-3K sorbent are produced [57].

Figure 4 shows micrographs of FNS (A) and Termoksid-35 (B) sorbent granule cross-sections.

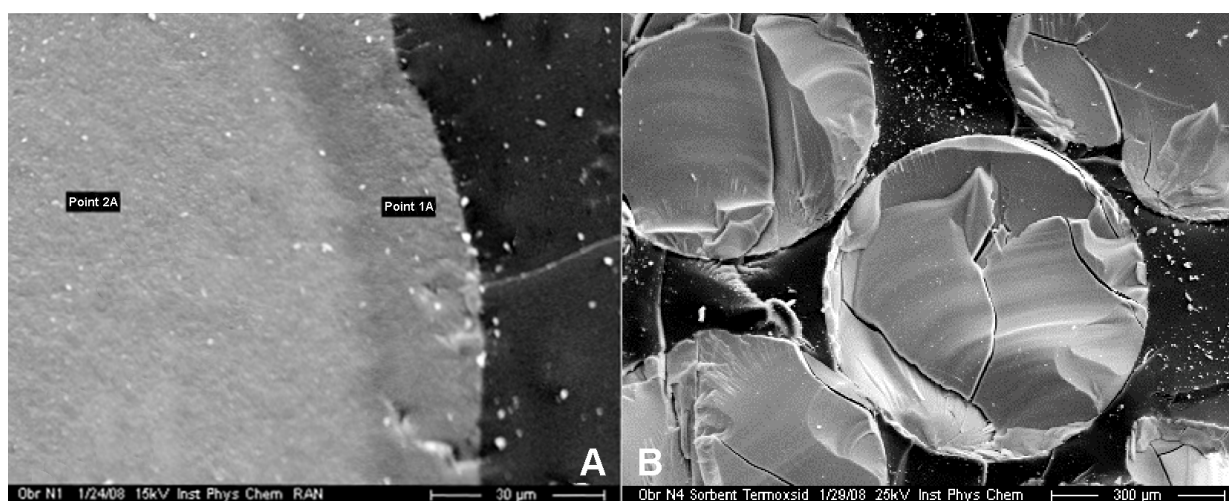


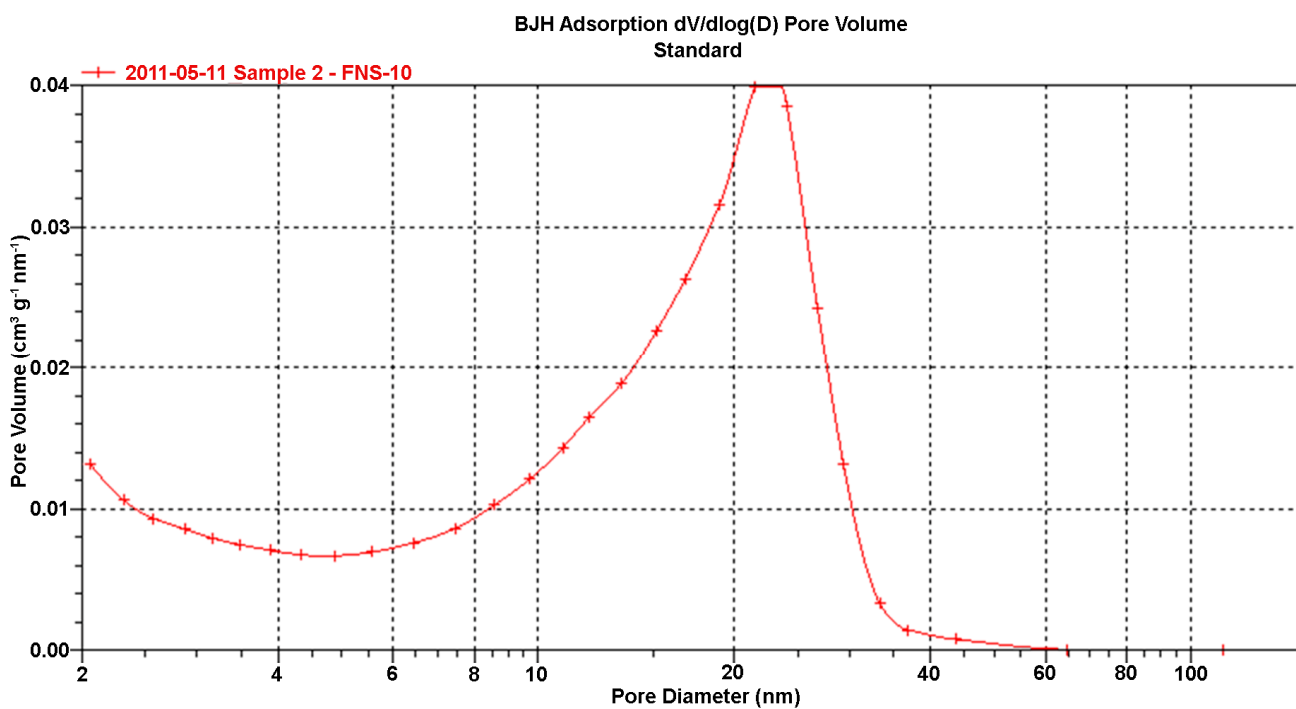
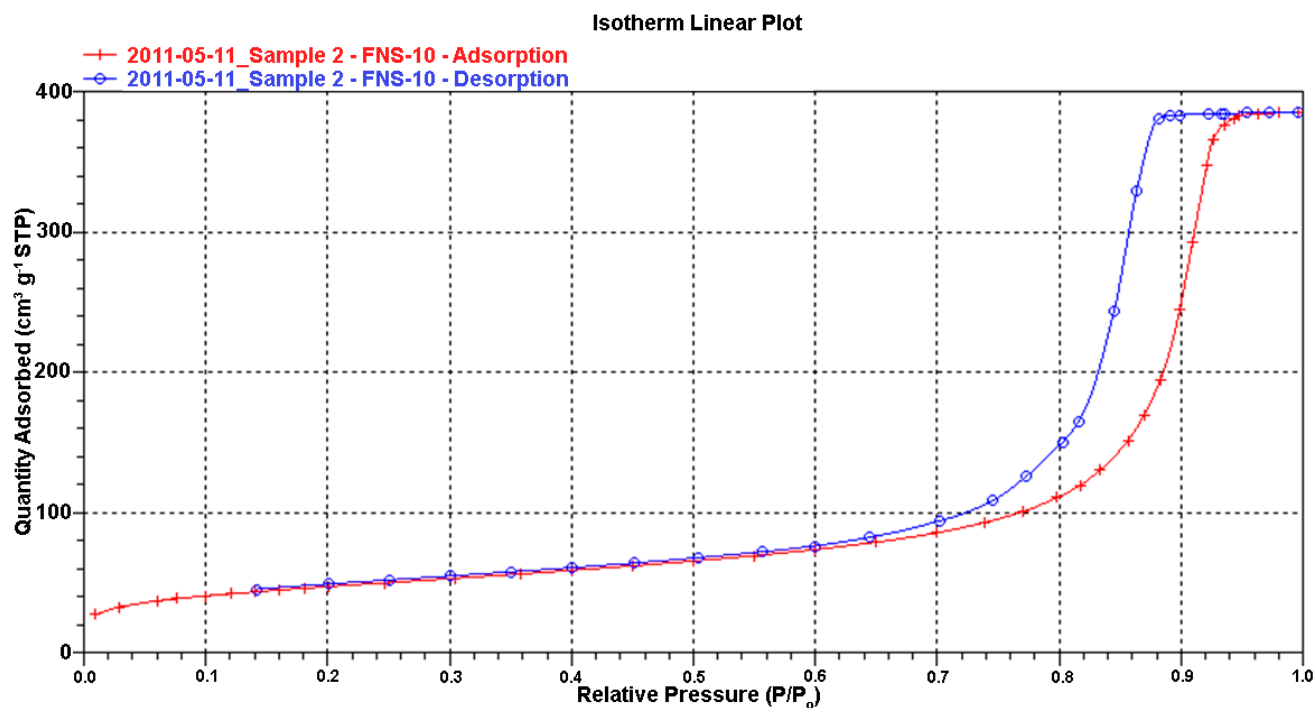
Figure 4. Scanning electron micrograph/image of FNS (A) and Termoksid-35 (B) sorbent granules' cross-sections (SEM analysis data).

The micrograph shows that for FNS sorbent, the nickel ferrocyanide phase is mainly concentrated on the external surface of the carrier granule. In photo 4A, the boundary of the nickel–potassium ferrocyanide layer is clearly visible.

The X-ray spectrometric microanalysis was used for determining the content of silica-gel carrier by Si and the nickel–potassium ferrocyanide phase of the composition $\text{K}_{0.68}\text{Ni}_{1.66}\text{Fe}(\text{CN})_6$ -by Ni and Fe. The measurements were performed on the surface (Point 1A) and in the center of the granule (Point 2A). The results obtained showed that molar ratios of Si/Fe and Si/Ni in Point 1A were 48.6 and 41.1, and 59.4 and 60.9 in Point 2A, respectively. It indicated that the nickel ferrocyanide phase was, for the most part, concentrated on the external surface of the granule.

In the Termoksid-35 sorbent, the ferrocyanide phase is uniformly distributed over the entire volume of the granule. In the case of the Thermoxide 35 sorbent, the ratios of the sorbent matrix component (Zr) to the sorption phase components (Fe, Ni) over the entire volume of the granule remain almost constant, which indicates the uniform distribution of nickel ferrocyanide in the sorbent phase.

The low-temperature nitrogen adsorption method was used to determine the porous structure of the FNS and Termoksid-35 sorbents. Adsorption isotherms and pore size distribution for FNS and Termoksid-35 sorbents are shown in Figures 5–8, respectively.



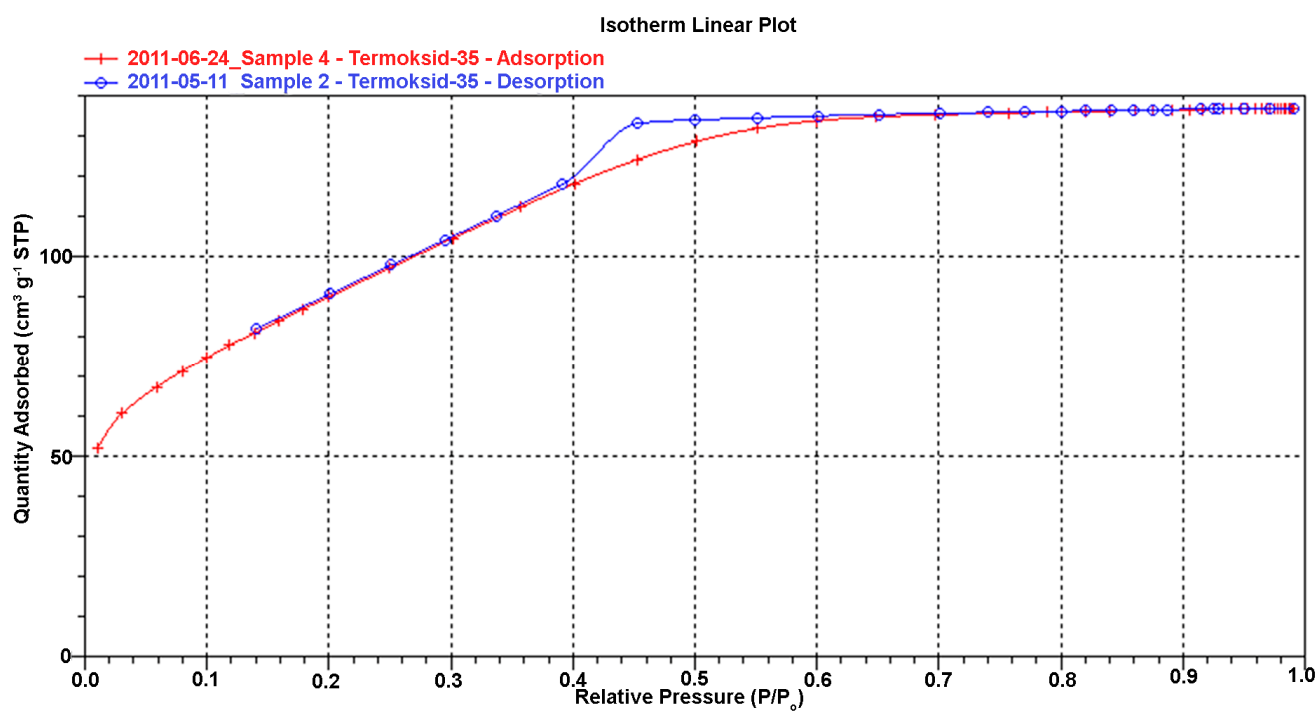


Figure 7. Nitrogen (N_2) adsorption/desorption isotherms of Termoksid-35 sorbent. X-axis is the p/p_0 —the relative pressure of the nitrogen gas; p_0 is the saturated gas pressure, Pa; Y-axis is the amount of adsorbed nitrogen gas, $cm^3 g^{-1}$ of the sorbent.

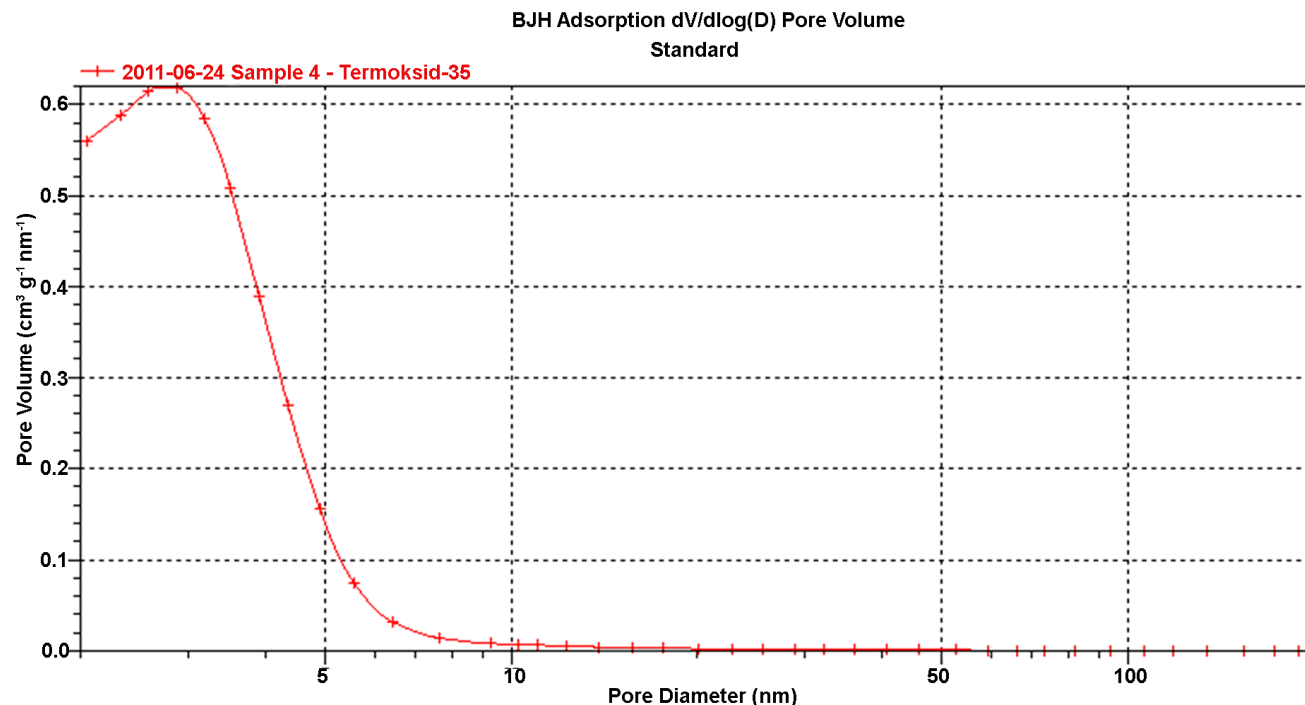


Figure 8. BJH pore size distribution of Termoksid-35 sorbent. X-axis is the pore diameter, nm; Y-axis is the volume of pores of a specific diameter, $cm^3 g^{-1}$ of the sorbent.

Figures 5–8 demonstrate the differences in the porous structure of the FSS and Termoksid 35 sorbents. The presented isotherms show that the FSS sorbent synthesized by chemical modification of large-pore silica gel has larger pores than the Termoksid 35 sorbent synthe-

sized by the sol-gel method. The above differences are reflected in the kinetic parameters of cesium sorption on these sorbents given in the paper.

Unfortunately, the characteristics of the analytical instruments available did not allow us to determine pores with a size below 2 nm. Again, micro- and mesopores in the sorbent are responsible only for the transport of absorbed ions to the phase boundary. The ion exchange itself occurs due to the replacement of mobile ions of the crystal lattice by the ions in the liquid phase. As mentioned above, the size of the entrance windows in transition metal ferrocyanides is 3.3–3.5 Å (0.33–0.35 nm), which is a good match to the size of the cesium ion (0.35 nm).

Characteristics of the porous structure for ferrocyanide sorbents under study, calculated from the adsorption isotherms, are given in Table 2.

Table 2. Characteristics of the porous structure for FNS and Termoksid-35 sorbents.

No.	Characteristics	Unit of Measurement	Value of the Characteristic	
			FNS	Termoksid-35
1	Type of the adsorption isotherm according to IUPAC	-	IV	IV
2	Specific surface area, by BET	m ² g ⁻¹	167 ± 2	328 ± 4
3	Specific volume of pores below 300 nm in diameter	cm ³ g ⁻¹	0.60 ± 0.01	0.21 ± 0.01
4	Specific volume of micropores	cm ³ g ⁻¹	0.04 ± 0.01	0.08 ± 0.01
5	Prevailing pore diameter	nm	23 ± 1	2.8 ± 0.3

The results presented in Table 2 showed that the FNS sorbent largely inherited the macroporous structure of the initial silica gel carrier used for the synthesis. The specific volume of macropores in the FNS sorbent was almost three times as high as in the Termoksid-35 sorbent. Moreover, the presence of macropores in the composition of the FNS sorbent provided higher kinetic characteristics during the sorption of cesium. The half-time of exchange during the sorption of tracer ¹³⁷Cs was 200 ± 20 and 120 ± 10 s, and the internal diffusion coefficient values of ¹³⁷Cs were (3.3 ± 0.8) × 10⁻¹² and (7.8 ± 1.5) × 10⁻¹² m² s⁻¹, on Termoksid-35 and FNS sorbents, respectively [58].

During the sorption of ⁹⁰Sr in the presence of calcium ions, maximum selectivity was observed on the manganese (III, IV) oxyhydrate-based MDM sorbent. For the other studied sorbents, strontium sorption was much less efficient because of the competition from calcium ions. In the MDM sorbent, the best match was observed between the sizes of the sorbent crystal lattice's entrance windows (2.850 Å) and the diameter of the Sr²⁺ ion (2.40 Å). For comparison, the diameter of the Ca²⁺ ion is 2.08 Å.

The sorption selectivity to ⁹⁰Sr in the presence of calcium ions on the MDM sorbent is also related to the "zeolite" effect. The MDM sorbent possesses a hexagonal symmetry birnessite-like structure with the crystal lattice parameters of a = 2.850 and C = 7.05–7.16 Å [59]. The strong effect of calcium ions on strontium sorption is related to the relatively small difference in the ionic radii of Ca²⁺ and Sr²⁺ ions of 1.04 and 1.20 Å, respectively. The porous structure of the MDM sorbent is represented by mesopores with a predominant pore diameter of 6–8 nm and a specific surface area of 220–240 m² g⁻¹.

The results obtained allowed us to propose the most effective types of sorbents for removing cesium and strontium radionuclides from radioactively contaminated natural water and technogenic liquid waste.

In case of radiation accidents, low salt-bearing fresh water and groundwater become contaminated with cesium and strontium radionuclides. The tests on removing ¹³⁷Cs and ⁹⁰Sr radionuclides from the water of Moscow River, Russia, were run to determine the efficiency of various sorbents studied for decontaminating this type of natural water. The chemical composition of river water was, mg dm⁻³: Na⁺: 6–8; K⁺: 4–5; Mg²⁺: 15–17; Ca²⁺:

52–56; Cl^- : 6–8; SO_4^{2-} : 36–38; HCO_3^- : 200–205; total salt content of 310–330; total hardness of 3.6–3.8 mg-eqv dm^{-3} ; pH 7.6–7.8. Before the runs, the trace amounts of ^{137}Cs and ^{90}Sr radionuclides were added in about 10^5 Bq dm^{-3} to obtain a simulated feed solution. The K_d values of ^{137}Cs and ^{90}Sr from river water on various sorbents are given in Table 3.

Table 3. The distribution coefficient (K_d) values of ^{137}Cs and ^{90}Sr during sorption from river water on various sorbents.

Sorbent Name	Bent–Ru	Cl-UKR	Purolite C 100	NaA	MDM	FNS
K_d ^{137}Cs , $\text{cm}^3 \text{g}^{-1}$	2.5×10^4	1.8×10^4	1650	8500	-	2.4×10^4
K_d ^{90}Sr , $\text{cm}^3 \text{g}^{-1}$	330	580	1880	4400	8600	-

The results in Table 3 illustrate that inexpensive natural sorbents, namely bentonite clays, clinoptilolite, and diatomite, could decontaminate low salt-bearing natural water from ^{137}Cs rather effectively. Moreover, those sorbents in their sorption capacity were not inferior to much more expensive synthetic sorbents.

However, the efficiency of natural sorbents for decontamination from strontium significantly decreases because of the intense competition with foreign ions, primarily calcium. In this case, the most reasonable is the application of the manganese (III, IV) oxyhydrate-based MDM sorbent and the synthetic zeolite of A-type.

After the Fukushima-1 Nuclear Power Plant accident, the issue of decontaminating seawater from ^{137}Cs and ^{90}Sr radionuclides has acquired particular importance. The main difficulty in seawater processing is its high salt content of up to 35 g dm^{-3} . The tests aimed to determine the set of sorbents most effective for solving the issue were performed on the sorption of ^{137}Cs and ^{90}Sr from simulated seawater. The simulant composition was as follows: g dm^{-3} : Na^+ : 10.29; K^+ : 0.38; Mg^{2+} : 1.23; Ca^{2+} : 0.39; Sr^{2+} : 0.0074; Cl^- : 18.51; SO_4^{2-} : 2.59; HCO_3^- : 0.123; Br^- : 0.064; H_3BO_3 : 0.024, total salt content: 34.0; pH 7.8 [60]. Prior to the experiments, about 10^5 Bq dm^{-3} of the ^{137}Cs and ^{90}Sr radionuclide tracers were added to the feed solution. The K_d values of ^{137}Cs and ^{90}Sr from seawater on various sorbents are given in Table 4.

Table 4. The distribution coefficient (K_d) values of ^{137}Cs and ^{90}Sr during sorption from seawater on various sorbents.

Sorbent Name	Bent–Ru	Cl-UKR	NaA	MDM	FNS	SRM-Sr
K_d ^{137}Cs , $\text{cm}^3 \text{g}^{-1}$	3500	1700	280	<10	1.1×10^4	<10
K_d ^{90}Sr , $\text{cm}^3 \text{g}^{-1}$	<10	<10	<10	590	<10	4.0×10^4

The results obtained during the sorption of ^{137}Cs from seawater showed that applying natural sorbents for the purpose was much less practical than synthetic inorganic sorbents, the ferrocyanide sorbents being the most effective.

For the decontamination of seawater from ^{90}Sr , it appeared most reasonable to use the barium silicate-based sorption-reagent material SRM-Sr; under the conditions given, it exhibited maximum efficiency in removing ^{90}Sr [61].

3. Materials and Methods

The sorption-selective characteristics of different sorbent types were evaluated by determining distribution coefficients (K_d) of tracer ^{137}Cs and ^{90}Sr radionuclides. The K_d value constitutes the main thermodynamic characteristic of the sorbent during the sorption of tracer amounts. In the range of tracer concentrations, the K_d value depends neither on the solid-to-liquid phase ratio nor the initial activity of the solution. This was reported in many publications on the sorption studies of sorbents' characteristics [24,25,47].

The experiments were run under batch conditions by mixing a 0.1 g weighed portion of the sorbent with a 20 cm³ aliquot of the feed solution containing ¹³⁷Cs and ⁹⁰Sr for 24 h. Further, the sorbent was filtered off through a paper filter of a “blue tape” type with a pore size of 2–3 micrometers, and the filtrate was analyzed for the specific activity of the radionuclide under study.

K_d values were calculated using the results of analyses according to the formula:

$$K_d = (A_0 - A_f) / A_f \times V_1 / m_s, \quad (1)$$

where A₀, A_f denoted the specific activity of the adsorbed radionuclide in the feed solution and filtrate, respectively, Bq dm⁻³;

V₁ is the liquid phase volume, cm³;

m_s is the sorbent mass, g.

Sorption of ¹³⁷Cs was performed from an aqueous 0.1 mol dm⁻³ NaNO₃ solution, pH 6.0; ⁹⁰Sr was adsorbed from an aqueous 0.01 mol dm⁻³ CaCl₂ solution, pH 6.0. The simulated feed solution for the experiments was prepared by adding about ~10⁵ Bq dm⁻³ of ¹³⁷Cs and ⁹⁰Sr radionuclides.

The sorbents examined in our studies are listed below.

- Purolite C 100—a gel-type strongly acidic sulfonic cation exchanger. Grain size was 0.315–1.25 mm, manufactured by the “Purolite” Company, UK;
- Bent-Ru is bentonite clay, Belgorod region, Russia;
- Bent-Gr is bentonite clay, Milos Island, Greece;
- Cl-UKR is clinoptilolite of the Sokirnitsa deposit, Ukraine;
- Cl-RUS is clinoptilolite of the Kholinsky deposit, Chita Region, Russia.
- NaA is sodium form of the type A zeolite, TU 2163-003-15285215-2006, manufactured by Ishimbay Specialized Chemical Plant of Catalysts (ISCPC), Bashkiria, Russia;
- NaX is sodium form of the type X zeolite, TU 2163-077-05766575-99, manufactured by Ishimbay Specialized Chemical Plant of Catalysts (ISCPC), Bashkiria, Russia;
- Termoksid-3K is spheric-shaped granulated zirconium oxyhydrate, manufactured by the JSC “Termoksid,” Russia;
- MDM is manganese (III, IV) oxide-based granulated sorbent, TU 2641-001-51255813-2007, manufactured by the Frumkin Institute of Physical Chemistry and Electrochemistry of the Russian Academy of Sciences (IPCE RAS), Moscow, Russia;
- Termoksid-3A is spheric-shaped granulated zirconium phosphate, manufactured by the JSC “Termoksid,” Russia;
- Termoksid-35 is spheric-shaped granulated nickel-potassium ferrocyanide on a zirconium oxyhydrate carrier, the ferrocyanide phase content is 28–32 wt.%, manufactured by the JSC “Termoksid,” Russia
- FNS is granulated nickel-potassium ferrocyanide on a silica gel carrier, the ferrocyanide phase content is 8–10 wt.%, manufactured by the IPCE RAS, Moscow, Russia;
- FND is finely dispersed nickel-potassium ferrocyanide on a natural aluminosilicate carrier, the ferrocyanide phase content is 15–20 wt.%, manufactured by the IPCE RAS, Moscow, Russia;
- SRM-Sr is granular sorption-reagent barium silicate-based material, granule size of 0.25–3.0 mm, the specific surface area of 326 m² g⁻¹; manufactured at the Institute of Chemistry, Far Eastern Branch of the Russian Academy of Sciences, Vladivostok, Russia;
- BAU is granulated activated birch wood-based carbon. Granule size of 1.2–3.6 mm, 1.2–3.6 mm, bulk density of 0.12 g cm⁻³, the specific surface area of 700–800 m² g⁻¹; micropores’ volume of 0.22–0.25 cm³ g⁻¹, mesopores’ volume of 0.08–0.10 cm³ g⁻¹, macropores’ volume of 1.35–1.45 cm³ g⁻¹, manufactured by the NPO “Sorbent,” Russia;
- NWC is a granulated activated coconut shell-based carbon. Granule size of 0.42–1.7 mm, bulk density of 0.18–0.52 g cm⁻³, a specific surface area of 350–400 m² g⁻¹; the micropores’ volume of 0.33–0.35 cm³ g⁻¹, mesopores’ volume of 0.03–0.05 cm³ g⁻¹,

macropores' volume of less than $0.01 \text{ cm}^3 \text{ g}^{-1}$, the adsorption capacity of 240 mg g^{-1} , produced by NWCarbon (India).

The specific activity of ^{137}Cs and ^{90}Sr radionuclides in solutions was measured by a multipurpose α - β - γ SKS-50M spectrometer (Green Star Technologies, Moscow, Russia). The γ -channel was equipped with a CsI scintillation detector having the following parameters: the energy resolution of 8 keV, efficiency of 0.08 counts per quantum, and measurement error not higher than 10%. The measurement geometry was a glass beaker of 60 mm diameter and 20 mm height. The β -channel was equipped with a BDEB-70 scintillation detector, an energy range of 50–3500 keV, an energy resolution of 15 keV, and a measurement error not higher than 10%. The measurement geometry was presented by a stainless steel cup of 50 mm diameter and 3 mm height.

The internal structure of the granulated sorbents was analyzed by scanning electron microscopy and X-ray spectrometric microanalysis using a JSM-V3 electron microscope (Japan) equipped with an EDX option "JEOL" ("Getac," Germany). The sample preparation procedure was as follows. The surface of the sample cleavage was used for examination. A piece about 1 cm in size was chipped from the sorbent granule. A thin layer of graphite was applied to its surface; the graphite deposition process occurred in a vacuum chamber equipped with a rotating cathode and graphite anode. A piece of the granule was attached to the cathode, the air was evacuated out of the chamber, and an electric potential was applied between the cathode and anode. The graphite particles detaching from the anode were deposited on the sample. The rotating cathode ensured all the surfaces of the sample were graphite-plated.

The mineral composition of clays was determined by X-ray diffraction using an ULTIMA-IV diffractometer, Rigaku, Japan with the new generation's DTex/Ultra semiconductor detector. The operating mode was 40 kV voltage, 40 mA current, copper anode, nickel filter, measurement scan range 3 – $65^\circ 2\theta$, scan speed $3^\circ 2\theta/\text{min}$ and pitch $0.02^\circ 2\theta$, fixed system of focusing slits.

Morphological characteristics of clay minerals were studied using a TITAN 80-300 TEM/STEM transmission electron microscope.

A Quadrasorb SI/Kr setup was used to determine the specific surface area at the temperature of liquid nitrogen (77.35 K). A 99.999% pure nitrogen gas was used as an adsorbate. The surface was calculated using the BET method, and several isotherm points in the P/P_s range from 0.05 to 0.30. The samples were preliminarily dried in a vacuum unit at 100°C for 5–24 h, depending on the properties of the initial samples.

4. Conclusions

In this paper, the application of adsorption methods for decontaminating liquid radioactive waste (LRW) and radioactively contaminated natural water from radioactive elements, primarily long-lived cesium, and strontium radionuclides is discussed. These radionuclides represent the most significant ecological threat to humans and the environment because of their long half-life of about 30 years and high radiotoxicity.

Analysis of the available scientific and technical literature allowed us to conclude that the methods of physical adsorption, as well as ion exchange on organic ion exchange resins, are not effective enough to remove cesium and strontium radionuclides from aqueous solutions because of a limited sorption selectivity in the presence of interfering cations. The most effective for the purpose are inorganic sorbents, which, compared to organic ion exchangers, have an increased selectivity to cesium and strontium ions.

Sorption of cesium and strontium radionuclides from aqueous solutions takes place by the mechanism of ion exchange between ions in the liquid phase and in the sorbent phase. In case of the physical adsorption, the absorption of solution components occurs due to the intermolecular interaction between the surface and absorbed ions (van der Waals forces), and the components are predominantly adsorbed in the molecular, rather than ionic form. Because conventional adsorbents, for example, active carbons, have a small count of ion-exchange groups on their surface, the sorption of ionic species of cesium and

strontium radionuclides on them is extremely low. It was confirmed by the experimental results obtained.

Sorption of cesium and strontium radionuclides on organic ion exchangers occurs due to electrostatic interaction between ions in solution and the ion exchanger matrix. Because the difference in the electrostatic interaction of ions of the same charge is small, the selectivity of cesium sorption in the presence of sodium ions, similar to that of strontium in the presence of calcium ions, is relatively small.

An increased selectivity of inorganic sorbents is associated with the so-called “zeolite” effect. When the sizes of the input windows of the crystalline phase and absorbed ions are close, the sorption occurs due to a stronger dispersion interaction between the absorbed ions and the sorbent matrix.

The efficiency of various sorption materials in relation to cesium and strontium radionuclides was evaluated using the standard technique developed for determining the distribution coefficient (K_d) values of ^{137}Cs and ^{90}Sr radionuclide tracers in solutions of sodium and calcium salts, the bulk components of LRW, and natural water. Under this study, the K_d values of ^{137}Cs and ^{90}Sr obtained for a wide range of different sorption materials enabled a justified choice of the most effective sorbents for removing highly toxic radionuclides of cesium and strontium from radioactively contaminated natural water and technogenic liquid waste.

It was also found that bentonite clays and natural and synthetic zeolites are the best for decontaminating low-salt natural water from cesium radionuclides, whereas ferrocyanide sorbents are the choice for decontaminating high-salt-bearing solutions (seawater). The manganese (III, IV) oxyhydrate-based MDM sorbent is the most effective for removing strontium from natural water, and for seawater, the barium silicate-based SRM-Sr sorbent is the best.

Author Contributions: Conceptualization, methodology, writing—original draft preparation, V.V.M.; formal analysis, investigation, N.A.N.; investigation, V.O.K.; resources, writing—review and editing, E.A.K. All authors have read and agreed to the published version of the manuscript.

Funding: This research was supported by the Frumkin’ Institute of Physical Chemistry and Electrochemistry of the Russian Academy of Sciences and received no external funding or grant to assist in conducting the study and preparing the manuscript.

Data Availability Statement: Data is available in a publicly accessible repository that does not issue DOIs. The link is <https://cloud.mail.ru/public/fZor/bhFo5Lswy> (last accessed on 20 February 2023).

Acknowledgments: The authors are willing to express their gratitude to the IPCE RAS Physical Investigation Methods Resource Sharing Center for assistance in diffraction and microscopic measurements.

Conflicts of Interest: The authors declare no conflict of interest. The authors have no relevant financial or non-financial interests to disclose. The authors have no competing interests to declare that are relevant to the content of this article. All authors certify that they have no affiliations with or involvement in any organization or entity with any financial interest or non-financial interest in the subject matter or materials discussed in this manuscript. The authors have no financial or proprietary interests in any material discussed in this article.

References

1. Looking Back to go Forward. In Proceedings of the an International Conference on Chernobyl, STI/PUB/1312. Vienna, Austria, 6–7 September 2005; ISBN 978–92–0–110807–4.
2. *The Fukushima Daiichi Accident*; Report by the Director General; STI/PUB/1710; IAEA: Vienna, Austria, 2015; ISBN 978–92–0–107015–9.
3. Abbasi, W.A.; Streat, M. Adsorption of uranium from aqueous solutions using activated carbon. *Separ. Sci. Technol.* **1994**, *29*, 1217–1230. [[CrossRef](#)]
4. Bulut, Y.; Tez, Z. Removal of heavy metals from aqueous solution by sawdust adsorption. *J. Environ. Sci.* **2007**, *19*, 160–166. [[CrossRef](#)] [[PubMed](#)]
5. Kutahyali, C.; Eral, M. Selective adsorption of uranium from aqueous solutions using activated carbon prepared from charcoal by chemical activation. *Sep. Purif. Technol.* **2004**, *40*, 109–114. [[CrossRef](#)]

6. Olorundare, O.F.; Krause, R.W.M.; Okonkwo, J.O.; Mamba, B.B. Potential application of activated carbon from maize tassel for the removal of heavy metals in water. *J. Phys. Chem. Earth* **2012**, *50–52*, 104–110. [[CrossRef](#)]
7. Someda, H.H.; Ezz El-Din, M.R.; Sheha, R.R.; El Naggar, H.A. Application of a carbonized apricot stone for the treatment of some radioactive nuclei. *J. Radioanal. Nucl. Chem.* **2002**, *254*, 373–378. [[CrossRef](#)]
8. Borai, E.H.; Hilal, M.A.; Attallah, M.F.; Shehata, F.A. Improvement of radioactive liquid waste treatment efficiency by sequential cationic and anionic ion exchangers. *Radiochim. Acta.* **2008**, *96*, 441–447. [[CrossRef](#)]
9. *Application of Ion Exchange Processes for the Treatment of Radioactive Waste and Management of Spent Ion Exchangers*; Technical Reports Series, No. 408; IAEA: Vienna, Austria, 2002; p. 202.
10. Ferrah, N.; Abderrahim, O.; Didi, M.A. Comparative study of Cd²⁺ ions sorption by both Lewatit TP 214 and Lewatit TP 208 resins: Kinetic, equilibrium and thermodynamic modelling. *Chem. J.* **2015**, *5*, 6–13.
11. Kadous, A.; Didi, M.A.; Villemin, D. Removal of uranium (VI) from acetate medium using Lewatit TP 260 resin. *J. Radioanal. Nucl. Chem.* **2020**, *288*, 553–561. [[CrossRef](#)]
12. Venkatesan, K.A.; Shyaqemla, K.V.; Antony, M.P.; Srinivasan, T.G.; Vasudeva, P.R. Batch and dynamic extraction of uranium from nitric acid medium by commercial phosphonic acid resin Tulsion CH-96. *J. Radioanal. Nucl. Chem.* **2008**, *275*, 563–570. [[CrossRef](#)]
13. Cheira, M.F.; Atia, B.M.; Kouraim, M.N. Uranium(VI) recovery from acidic leach liquor by Ambersep 920U SO₄ resin: Kinetic, equilibrium and thermodynamic studies. *J. Radiat. Res. Appl. Sci.* **2017**, *10*, 307–319. [[CrossRef](#)]
14. Kosari, M.; Seprehrian, H.; Ahangari, R. Uranium Removal from Aqueous Solution Using Ion-exchange Resin DOWEX 2 × 8 in the Presence of Sulfate Anions. *Int. J. Eng.* **2016**, *29*, 1677–1683. [[CrossRef](#)]
15. Hartmann, E.; Geckeis, H.; Rabung, T.; Lützenkirchen, J.; Fanghänel, T. Sorption of radionuclides onto natural clay rocks. *Radiochim. Acta.* **2008**, *96*, 699–707. [[CrossRef](#)]
16. Lujaniene, G.; Šapolaite, J.; Radžiute, E.; Ščiglo, T.; Beneš, P.; Štamberg, K.; Vopalka, D. Effect of natural clay components on sorption of Cs, Pu and Am by the clay. *J. Radioanal. Nucl. Chem.* **2010**, *286*, 353–359. [[CrossRef](#)]
17. Milyutin, V.V.; Gelis, V.M.; Nekrasova, N.A.; Kononenko, O.A.; Vezentsev, A.I.; Volovicheva, N.A.; Korol'kova, S.V. Sorption of Cs, Sr, U and Pu radionuclides on natural and modified clays. *Radiochemistry* **2012**, *54*, 75–78. [[CrossRef](#)]
18. Sprynskyy, M.; Kovalchuk, I.; Buszewski, B. The separation of uranium ions by natural and modified diatomite from aqueous solution. *J. Hazard. Mater.* **2010**, *181*, 700–707. [[CrossRef](#)] [[PubMed](#)]
19. Borai, E.H.; Harjula, R.; Paajanen, A. Efficient removal of cesium from low-level radioactive liquid waste using natural and impregnated zeolite minerals. *J. Hazard. Mater.* **2009**, *172*, 416–422. [[CrossRef](#)]
20. Misaelides, P. Application of natural zeolites in environmental remediation: A short review. *Microporous Mesoporous Mater.* **2001**, *144*, 15–18. [[CrossRef](#)]
21. Osmanoglu, A.E. Treatment of radioactive liquid waste for sorption on natural zeolite in Turkey. *J. Hazard. Mater.* **2009**, *137*, 332–335. [[CrossRef](#)]
22. Kwon, S.; Choi, Y.; Sigh, B.K. Selective and rapid capture of Sr²⁺ with LTA zeolites: Effect of crystal sizes and mesoporosity. *Appl. Surf. Sci.* **2020**, *506*, 15. [[CrossRef](#)]
23. Sigh, B.K.; Tomar, R.; Kumar, S.; Jain, A.; Tomar, B.S.; Manchanda, V.K. Sorption of ¹³⁷Cs, ¹³³Ba and ¹⁵⁴Eu by synthesized sodium aluminosilicate (Na-AS). *J. Hazard. Mater.* **2010**, *178*, 771–776. [[CrossRef](#)]
24. Hua, M.; Zhang, S.; Pan, B.; Zhang, W.; Lv, L.; Zhang, Q. Heavy metal removal from water/wastewater by nanosized metal oxides: A Review. *J. Hazard. Mater.* **2012**, *211–212*, 317–331. [[CrossRef](#)]
25. Kuznetsova, V.A.; Generalova, V.A. The study of sorption properties of iron, manganese, titanium, aluminum and silicone oxides with respect to ⁹⁰Sr and ¹³⁷Cs. *Radiochemistry* **2000**, *42*, 154–157.
26. Valsala, T.P.; Joseph, A.; Sonar, N.L.; Sonavane, M.S.; Shah, J.G.; Raj, K.A.; Venugopal, V. Separation of strontium from low level radioactive waste solutions using hydrous manganese dioxide composite materials. *J. Nucl. Mater.* **2010**, *404*, 138–143. [[CrossRef](#)]
27. Singh, B.K.; Tomar, R.; Kumar, S.; Kar, A.S.; Tomar, B.S.; Ramanathan, S.; Manchanda, V.K. Role of the humic acid for sorption of radionuclides by synthesized titania. *Radiochim. Acta* **2014**, *102*, 255–261. [[CrossRef](#)]
28. Ivanets, A.; Milyutin, V.; Shashkova, I.; Kitikova, N.; Nekrasova, N.; Radkevich, A. Sorption of stable and radioactive Cs(I), Sr(II), Co(II) ions on Ti-Ca-Mg phosphates. *J. Radioanal. Nucl. Chem.* **2020**, *324*, 1115–1123. [[CrossRef](#)]
29. Thakkar, R.; Chudasama, U. Synthesis and characterization of zirconium titanium phosphate and its application in separation of metal ions. *J. Hazard. Mater.* **2009**, *172*, 129–137. [[CrossRef](#)]
30. Decaillon, J.G.; Andres, Y.; Mokili, B.M.; Abbe, J.C.; Tournoux, M.; Patarin, J. Study of the ion exchange selectivity of layered titanosilicate Na₃(Na,H)Ti₂O₂[Si₂O₆]₂ × 2H₂O, AM-4, for strontium. *Solvent Extr. Ion Exch.* **2002**, *20*, 273–291. [[CrossRef](#)]
31. Hobbs, D.T.; Barnes, M.J.; Pulmano, R.L.; Marshall, K.M.; Edwards, T.B.; Bronikowski, M.G.; Fink, S.D. Strontium and Actinide Separations from High Level Nuclear Waste Solutions Using Monosodium Titanate. 1. Simulant Testing. *Sep. Sci. Technol.* **2005**, *40*, 3093–3111. [[CrossRef](#)]
32. Lehto, J.; Brodtkin, L.; Harjula, R.; Tusa, E. Separation of radioactive strontium from alkaline nuclear waste solutions with the highly effective ion exchanger SrTreat. *Nucl. Technol.* **1999**, *127*, 81–87. [[CrossRef](#)]
33. Milyutin, V.V.; Nekrasova, N.A.; Yanicheva, N.Y.; Kalashnikova, G.O.; Ganicheva, Y.Y. Sorption of cesium and strontium radionuclides onto crystalline alkali metal titanosilicates. *Radiochemistry* **2017**, *59*, 65–69. [[CrossRef](#)]
34. Park, Y.; Shin, W.S.; Reddy, G.S.; Shin, S.J.; Choi, S.J. Use of nanocrystalline silicotitanate for the removal of Cs, Co and Sr from low-level liquid radioactive waste. *J. Nanoelectron. Optoelectron.* **2010**, *5*, 238–242. [[CrossRef](#)]

35. Solbra, N.; Allison, S.; Waite, S.; Mihalovsky, A.; Bortun, L.; Clearfield, A. Cesium and strontium ion exchange on the framework titanium silicate $M_2Ti_2O_3SiO_4 \times nH_2O$ ($M = H, Na$). *Environ. Sci. Technol.* **2001**, *35*, 626–629. [[CrossRef](#)] [[PubMed](#)]
36. Liu, H.D.; Li, F.Z.; Zhao, X.; Yun, G.C. Preparing high-loaded potassium cobalt hexacyanoferrate/silica composite for radioactive wastewater treatment. *Nucl. Technol.* **2009**, *165*, 200–208. [[CrossRef](#)]
37. Milonjic, I.; Bispo, M.; Fedoroff, C.V. Sorption of cesium on cooper hexacyanoferrate/polymer/silica composites in batch and dynamic conditions. *J. Radioanal. Nucl. Chem.* **2002**, *252*, 497–501. [[CrossRef](#)]
38. Milyutin, V.V.; Kononenko, O.A.; Mikheev, S.V.; Gelis, V.M. Sorption of cesium on finely dispersed composite ferrocyanide sorbents. *Radiochemistry* **2010**, *52*, 281–283. [[CrossRef](#)]
39. Chaptman, D.M.; Roe, A.L. Synthesis, characterization and crystal chemistry of microporous titanium-silicate materials. *Zeolites* **1990**, *10*, 730–737. [[CrossRef](#)]
40. Duff, M.C.; Hanter, D.B.; Hobbs, D.T.; Fink, S.D.; Dai, Z.; Bradey, J.P. Mechanism of strontium and uranium removal from high-level radioactive waste simulant solution by the sorbent monosodium titanate. *Environ. Sci. Technol.* **2007**, *38*, 5201–5207. [[CrossRef](#)] [[PubMed](#)]
41. Lee, J.; Park, S.M.; Jeon, E.K.; Baek, K. Selective and irreversible adsorption mechanism of cesium on illite. *Appl. Geochem.* **2017**, *85*, 188–193. [[CrossRef](#)]
42. Leontieva, G.V. Structural modification of manganese (III, IV) oxides in synthesis of sorbents selective for strontium. *Russ. J. Appl. Chem.* **1997**, *70*, 1615–1618.
43. Alby, D.; Charnay, C.; Heran, M.; Prelot, B.; Zajac, J. Recent developments in nanostructured inorganic materials for sorption of cesium and strontium: Synthesis and shaping, sorption capacity, mechanisms, and selectivity—A review. *J. Hazard. Mater.* **2018**, *344*, 511–530. [[CrossRef](#)]
44. Massoni, N.; Koch, R.J.; Hertz, A.; Campayo, L.; Moloney, M.P.; Mixture, S.T.; Grandjean, A. Structural effects of calcination on Cs-exchanged copper hexacyanoferrate $(Cs,K)_2CuFe(CN)_6$ loaded on mesoporous silica particles. *J. Nucl. Mater.* **2020**, *528*, 151887. [[CrossRef](#)]
45. Li, Y.L.; Zeidman, B.D.; Hu, S.Y.; Henager, C.H., Jr.; Besmann, T.M.; Grandjean, A. A physics-based mesoscale phase-field model for predicting the uptake kinetics of radionuclides in hierarchical nuclear wasteform materials. *Comput. Mater. Sci.* **2019**, *159*, 103–109. [[CrossRef](#)]
46. Abdel-Rahman, R.O.; Ibrahim, H.A.; Hanafy, M.; Abdel-Monem, N.M. Assessment of synthetic zeolite NaA-X as sorbing barrier for strontium in a radioactive disposal facility. *Chem. Eng. J.* **2010**, *157*, 100–112. [[CrossRef](#)]
47. Hassan, N.M.; Adu-Wusu, K.; Marra, J.C. Resorcinol—Formaldehyde adsorption of cesium from Hanford waste solutions. *J. Radioanal. Nucl. Chem.* **2005**, *262*, 579–586. [[CrossRef](#)]
48. Sergienko, V.I.; Avramenko, V.A.; Glushchenko, V.Y. Sorption Technology of LRW Treatment. *J. Ecotechnol. Res.* **1995**, *1*, 152.
49. Andryushchenko, N.D.; Safonov, A.V.; Babich, T.L.; Ivanov, P.V.; Konevnik, Y.V.; Kondrashova, A.A.; Proshin, I.M.; Zakharova, E.V. Sorption characteristics of materials of the filtration barrier in upper aquifers contaminated with radionuclides. *Radiochemistry* **2017**, *9*, 414–424. [[CrossRef](#)]
50. Fuks, L.; Herdzyk-Koniecko, I. Vermiculite as a potential component of the engineered barriers in low- and medium-level radioactive waste repositories. *Appl. Clay Sci.* **2018**, *161*, 139–150. [[CrossRef](#)]
51. Osipov, V.I.; Sokolov, V.N. Clays and their properties. Composition, structure, and formation of properties. *Moscow GEOS RF* **2013**.
52. Olphen, V. *Data Handbook for Clay Materials and other Non-Metallic Minerals*; Pergamon Press: Oxford, UK, 1979; Volume 28.
53. Cornell, R.M. Adsorption of cesium on minerals: A review. *J. Radioanal. Nucl. Chem.* **1993**, *171*, 483–500. [[CrossRef](#)]
54. Maskalchuk, L.N.; Milyutin, V.V.; Nekrasov, N.A.; Leontieva, T.G.; Baklay, A.A.; Belousov, P.E.; Krupskaya, V.V. Aluminosilicate Sorbents Based on Clay-Salt Slimes from JSC «Belaruskali» for Sorption of Cesium and Strontium Radionuclides. *Radiochemistry* **2020**, *62*, 381–386. [[CrossRef](#)]
55. Tananaev, I.V.; Seifer, G.B.; Kharitonov, Y.Y. The chemistry of ferrocyanides. *Moscow Nauka RF* **1971**.
56. Marhol, M. *Ion Exchangers in Analytical Chemistry*; Elsevier Scientific Pub. Co.: New York, NY, USA, 1982.
57. Sharygin, L.M. *Thermal Resistant Inorganic Sorbents*; UrO RAS: Ekaterinburg, Russia, 2012.
58. Milyutin, V.V.; Gelis, V.M.; Leonov, N.B. Kinetic sorption studies of cesium and strontium radionuclides by the sorbents of different classes. *Radiochemistry* **1998**, *40*, 418–420.
59. Feng, Q.; Kanoh, H.; Ooi, K. Manganese oxide porous crystals. *J. Mater. Chem.* **1999**, *9*, 319–333. [[CrossRef](#)]
60. Avramenko, V.A.; Zheleznov, V.V.; Kaplun, E.V.; Sokol'nitskaya, T.A.; Yukhkam, A.A. Sorption Recovery of Strontium from Seawater. *Radiochemistry* **2001**, *43*, 433–436. [[CrossRef](#)]
61. Avramenko, V.A.; Sergienko, V.I.; Sokol'nitskaya, T.A. Application of sorption-reagent materials in the technology of liquid radioactive waste treatment. *Theor. Found. Chem. Eng.* **2016**, *50*, 593–597. [[CrossRef](#)]

Disclaimer/Publisher's Note: The statements, opinions and data contained in all publications are solely those of the individual author(s) and contributor(s) and not of MDPI and/or the editor(s). MDPI and/or the editor(s) disclaim responsibility for any injury to people or property resulting from any ideas, methods, instructions or products referred to in the content.